Rapid Communications

System-size scan of D meson R_{AA} and v_n using PbPb, XeXe, ArAr, and OO collisions at energies available at the CERN Large Hadron Collider

Roland Katz,[1] Caio A. G. Prado,[2] Jacquelyn Noronha-Hostler,[3] and Alexandre A. P. Suaide[4]
[1]*SUBATECH, Université de Nantes, EMN, IN2P3/CNRS, 44307 Nantes, France*
[2]*Institute of Particle Physics, Central China Normal University (CCNU), Wuhan, Hubei 430079, China*
[3]*University of Illinois at Urbana-Champaign, Urbana, Illinois 61801, USA*
[4]*Instituto de Física, Universidade de São Paulo, Caixa Postale 66318, 05315-970 São Paulo, São Paulo, Brazil*

(Received 15 June 2020; accepted 2 September 2020; published 1 October 2020)

Experimental measurements indicate no suppression (e.g., $R_{\rm pPb} \approx 1$) but a surprisingly large D meson v_2 was measured in $p+$Pb collisions. In order to understand these results, we use Trento +v-USPhydro + DAB-MOD with event-by-event realistic hydrodynamic background to make predictions and propose a system size scan at the Large Hadron Collider (LHC) involving ^{208}PbPb, ^{129}XeXe, ^{40}ArAr, and ^{16}OO collisions. We find that the nuclear modification factor approaches unity as the system size is decreased, but nonetheless, in the 0–10% most central collisions, $v_2\{2\}$ is roughly equivalent regardless of system size. These results arise from a rather nontrivial interplay between the shrinking path length and the enhancement of eccentricities in small systems at high multiplicity. Finally, we also find a surprising sensitivity of D mesons $v_2\{2\}$ in 0–10% at $p_{\rm T} = 2$–10 GeV to the slight deformation of ^{129}Xe recently found at the LHC.

DOI: 10.1103/PhysRevC.102.041901

1. Introduction. The nature and properties of the smallest fluid known to humanity—the quark-gluon plasma—has pushed the boundaries of our understanding of fluid dynamics. Three significant signatures of the quark-gluon plasma are collective flow, strangeness enhancement, and suppression of hard probes. The first two signatures, collective flow and strangeness enhancement, have been measured in small asymmetric collisions, such as $p+$Pb, $d+$Au, and ^{3}HeAu [1–22]. Relativistic hydrodynamics manages to reproduce most flow observables in small systems well [23–31], although other scenarios that do not rely on relativistic hydrodynamics have been considered [32–35]. New experiments and measurements have been proposed in order to either confirm (or disprove) that relativistic hydrodynamics is the correct dynamical description in these tiny systems. For instance, polarized beams [36] and ultracentral deformed ion-ion collisions [37] both may distinguish between different scenarios in these light nuclei collisions.

The validity of event-by-event relativistic hydrodynamics remains to be studied in intermediate AA collisions across multiple types of ions. It was recently proposed for the Large Hadron Collider (LHC) energies to run a system size scan including ArAr and OO collisions [38] where a variety of hydrodynamic predictions have been performed [39–41]. More recently, a system size scan has also been proposed for the Relativistic Heavy Ion Collider (RHIC) energies as well [42].

Although collective flow experiment and theory comparisons are quite intriguing in small systems, we still lack a fundamental understanding of why jet and heavy flavor suppression is not measured in small systems (e.g., $R_{\rm pPb} \approx 1$ [43,44]). Predictions of XeXe R_{AA} have been performed in Refs. [45,46] (although only with the assumption of spherical ^{129}Xe), quarkonium predictions for $p+$A in Ref. [47] from the color glass condensate (CGC), preliminary results for photons in $p+$Pb, $p+$Au, $d+$Au, and ^{3}HeAu collisions were shown in Ref. [48], and previous $p+$Pb calculations in a variety of scenarios can be found in Refs. [49–51]. However, we are not aware of any predictions available for intermediate systems, such as ArAr/OO nor any current azimuthal anisotropy predictions assuming event-by-event relativistic hydrodynamics as the medium that hard probes pass through. Meanwhile, the CMS Collaboration has measured a significant D meson flow in $p+$Pb collisions [52], which is large but also somewhat suppressed compared to other identified particles. Additionally, the ATLAS Collaboration has measured a significant v_2 from heavy flavor μ's in $p+$Pb collisions [53]. It has also been suggested that the R_{AA}-to-v_2 puzzle may be a good testing bed for initial conditions [54]. Because D mesons are sensitive to equilibrium vs out-of-equilibrium dynamics (as shown in Fig. 10 from Ref. [55]) combined with the significant v_2 in small systems, they appear to be ideal candidates for understanding system size effects.

Whereas in the CGC scenario, one can reproduce the experimentally measured heavy flavor v_2 [47], no one has demonstrated in an initial condition + hydrodynamic + energy loss and Langevin scenario how such a large v_2 in small systems is compatible with $R_{AA} \to 1$. Here, we systematically study the effect of system size (by varying the colliding nuclei) on the nuclear modification factor R_{AA}, azimuthal anisotropies $v_n\{2\}$, and multiparticle cumulants $v_2\{4\}/v_2\{2\}$. To conduct this Rapid Communication, we use Trento [56] + v-USPhydro [57,58] + DAB-MOD [59] using the exact same soft

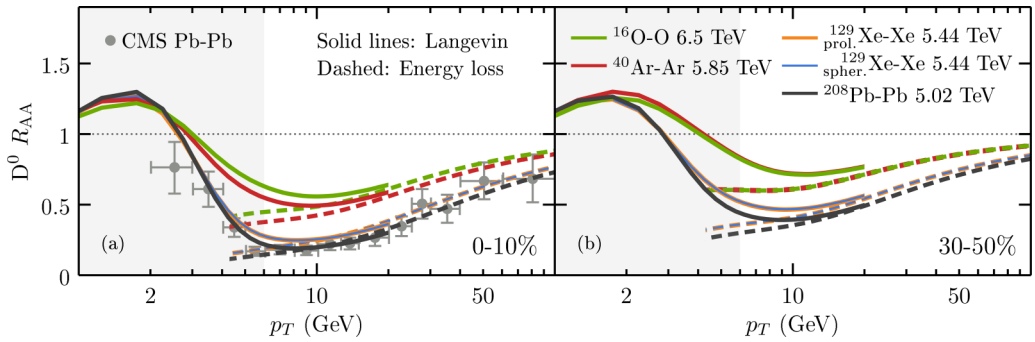

FIG. 1. D^0 meson R_{AA} for PbPb, XeXe with spherical and prolate initial nuclei, ArAr and OO collisions at the LHC top energies in (a) 0–10% and (b) 30–50% centrality classes. The gray (white) area indicates the p_T region where the Langevin (energy-loss) description is the most relevant.

sector event-by-event backgrounds as in Refs. [39,60,61] and both the Langevin "Moore and Teaney" and the "constant" energy loss set up from Ref. [62] that works well compared to PbPb data at low and high p_T's, respectively. We find that as the system size is shrunk $R_{AA} \to 1$, however, the $v_n\{2\}$'s have a rather nontrivial relationship with the system size that can only be understood with direct comparisons with the soft sector from Ref. [39]. Finally, we also find a nontrivial sensitivity to a deformed nucleons in intermediate $p_T = 2$–10-GeV D meson v_2 calculations, which is consistent with soft sector calculations [61].

2. Model description. In this Rapid Communication, we couple event-by-event hydrodynamical backgrounds in $2+1$ dimensions that fit the soft sector well to the heavy flavor code DAB-MOD [59,62]—a modular Monte Carlo simulation package developed to study D and B mesons—that samples heavy quarks using distributions from pQCD fixed-order next-to-leading-logs calculations [63,64]. Then, either a parametrized energy-loss model that includes energy-loss fluctuations (sampled from an underlying distribution) is used for the heavy quarks evolution or a relativistic Langevin model based on an input drag or diffusion coefficient. Once the decoupling temperature $T_d = 160$ MeV is reached, hadronization follows via a hybrid fragmentation and coalescence model from which the final nuclear modification factor can be reconstructed. In Ref. [62], it was shown for PbPb collisions that with the Langevin description using the purely collisional spatial diffusion coefficient model from Ref. [65] [with $D_s(2\pi T) = 2.23$], one obtains a reasonable description of experimental data at low $p_T \lesssim 5$ to 6 GeV, whereas for the high $p_T \gtrsim 5$-to-6-GeV sector, it was found that an energy-loss model works best [66]. However, the range of applicability for Langevin vs energy loss is not clear across system size and, therefore, we compare them across a somewhat wider range. The initial conditions + hydrodynamical backgrounds are identical to those used in Refs. [39,60,61] where the Trento initial conditions used the parameters $p = 0$, $k = 1.6$, and $\sigma = 0.51$ fm as established by a Bayesian analysis [67]. The parameters of the viscous hydrodynamic code v-USPhydro are $\tau_0 = 0.6$ fm, $\eta/s = 0.047$, $T_{\text{FO}} = 150$ MeV, which have been shown to fit well compared to experimental data. We test both a spherical ^{129}Xe nucleus and a prolate one (per the parametrization of the deformed Woods-Saxon in Refs. [61,68]).

One should note that, in our model, there is some ambiguity on the overall magnitude of R_{AA} in the absence of experimental data since we generally fix the scaling constant of the transport model using high-p_T R_{AA} in most central collisions. Thus, it is possible that there may be a system size dependence to this constant, whereas we use, here, for all systems, the value obtained in PbPb collisions. Furthermore, although we write $v_n\{2\}$ to indicate that this is a two-particle correlation—obtained via the scalar product method for cumulants—we also point out that one of these particles is a soft particle whereas the other is a heavy flavor hadron as has been discussed extensively in Refs. [59,69–72].

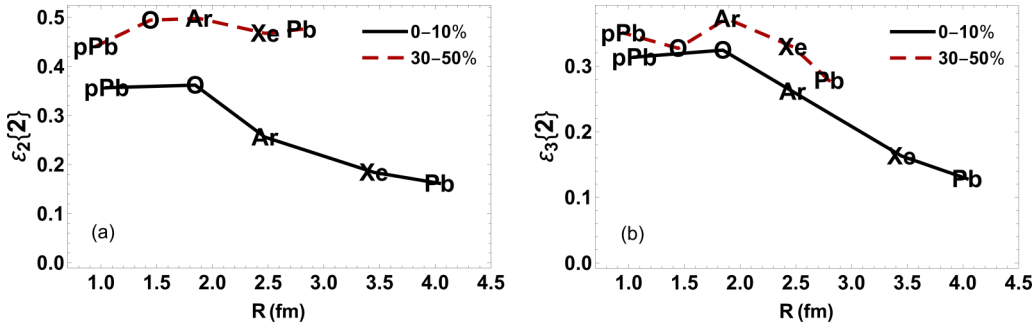

FIG. 2. (a) $\varepsilon_2\{2\}$ and (b) $\varepsilon_3\{2\}$ vs radius for PbPb, XeXe, ArAr, and OO collisions at the LHC top energies in 0–10% and 30–50% centrality classes.

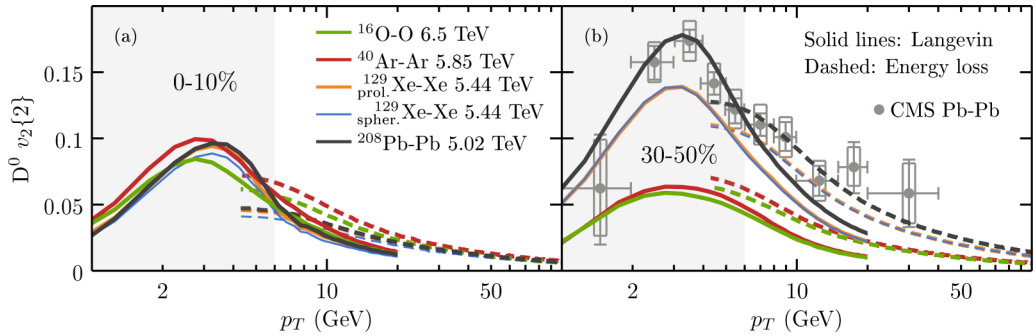

FIG. 3. D^0 meson $v_2\{2\}$ for PbPb, XeXe with spherical and prolate initial nuclei, ArAr, and OO collisions at the LHC top energies in (a) 0–10% and (b) 30–50% centrality classes. The gray (white) area indicates the p_T region where the Langevin (energy-loss) description is the most relevant.

3. Results. In small systems, it was found that the nuclear modification factor is consistent with unity within error bars [73–80]. However, it is not clear how R_{AA} changes with system size as one moves towards small systems: Does it smoothly increase as the size shrinks or does it suddenly jump to 1 at a certain critical size? Additionally, is the lack of light flavor jet suppression unique to asymmetric systems? These questions are precisely investigated in Fig. 1 where we show the R_{AA} of D mesons in 0–10% and 30–50% centrality classes. There are a number of conclusions that can be drawn from these results. First, 0–10% centralities are more sensitive to system size effects, whereas for 30–50% centralities, one cannot see a distinguishable difference between ArAr and OO, even though there is a clear difference in system size [39]. We note that R_{AA} is insensitive to any effects of a deformed nucleus regardless of the centrality class. Second, it is clear that $R_{AA} \to 1$ as the system size decreases, $(1 - R_{AA})$ being roughly proportional to the system initial radius $\approx A^{1/3}$ from $p_T \gtrsim 4$ GeV, which implies that we expect a smooth decrease in the suppression of hard probes as one decreases the system size, eliminating the idea of a sharp critical system size within our framework. However, for the smallest system size of OO collisions, there is still a rather important deviations from 1 at intermediate p_T. Indeed, the 0–10% centrality class can get a minimum close to $R_{AA} \approx 0.5$ at its minimum whereas the 30–50% centrality class has $R_{AA} \approx 0.7$ to 0.8. Extrapolating these results to $p+$Pb collisions—with radii of about two times smaller than OO collisions (see Fig. 2)—it is not obvious that the R_{AA} would reach unity enough to be consistent with $p+$Pb data. Finally, we find that Langevin and energy-loss R_{AA} converge at high p_T and the point of convergence occurs only at even higher p_T for smaller systems. In contrast, at intermediate $p_T \approx 5$–10 GeV, the Langevin model predicts significantly less suppression than energy loss. We also point out that the difference between energy loss vs Langevin in R_{AA} varies with system size due to different path-length dependences.

For the azimuthal anisotropies, it is important to understand that not only does the system size shrink, but also the geometrical shapes of the initial conditions change as well [39]. In Fig. 2, we plot the radius of the initial conditions R vs the eccentricities ε_n in the two centrality classes considered here: 0–10% and 30–50%. The systems coming from PbPb, XeXe, ArAr, and OO central collisions have both significantly different sizes and significantly different eccentricities: As one decreases the radius, the eccentricities increase. In contrast, midcentral collisions have roughly equivalent eccentricities and only vary in system size. Thus, the midcentral collisions give us a better insight into pure system size effects. However, one should caution that the D meson results from Ref. [5] are measured in central $p+$Pb collisions so, to some extent, they may experience both varying system size and eccentricities compared to large AA collisions.

The azimuthal anisotropies of hard probes can be useful too to study diffusion and energy loss [46,55,59,69,70,81–90]. In Fig. 3, the elliptical azimuthal anisotropies are shown for D mesons at 0–10% and 30–50% centralities. We find that when we hold $\varepsilon_2 \approx$ const. in the 30–50% centrality class the influence of the smaller system size plays a dramatic role in Fig. 3 for both descriptions of D dynamics where in small systems D mesons v_2 is significantly suppressed across all p_T's. Nevertheless, what is somewhat surprising is that $v_2\{2\}(p_T)$ of OO collisions is roughly equivalent to $v_2\{2\}(p_T)$ of ArAr collisions.

Now, that we have shown that the system size suppresses D meson v_2 when the eccentricities are held fixed, we can

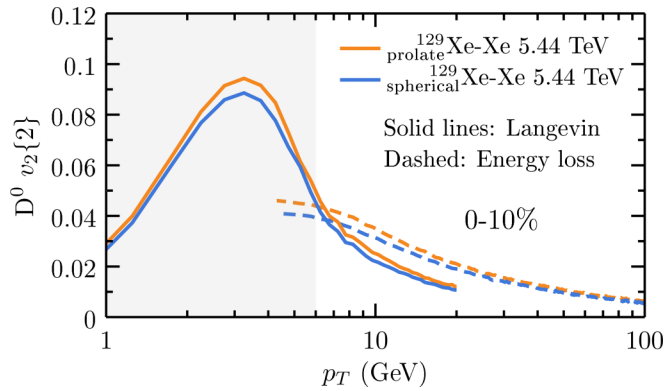

FIG. 4. D^0 meson $v_2\{2\}$ for XeXe collisions with spherical and prolate initial nuclei at the LHC top energies in the 0–10% centrality class. The gray (white) area indicates the p_T region where the Langevin (energy-loss) description is the most relevant.

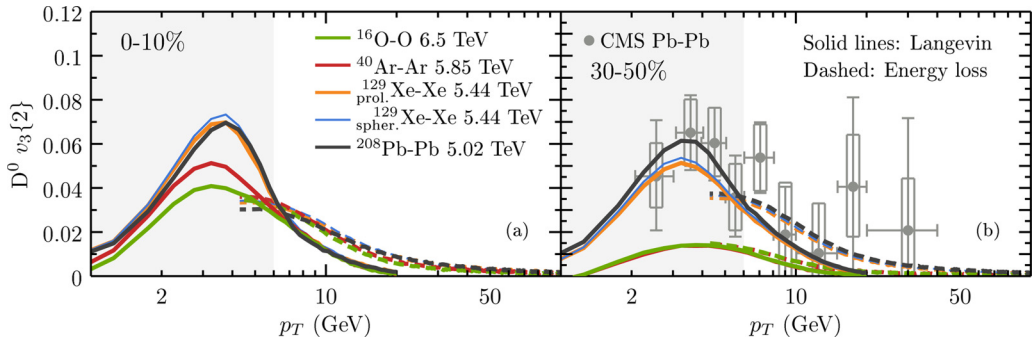

FIG. 5. D^0 meson $v_2\{2\}$ for PbPb, XeXe with spherical and prolate initial nuclei, ArAr, and OO collisions at the LHC top energies in (a) 0–10% and (b) 30–50% centrality classes. The gray (white) area indicates the p_T region where the Langevin (energy-loss) description is the most relevant.

understand the results in the 0–10% centrality class in Fig. 3 where v_2 is roughly equivalent regardless of system size. Additionally, v_2 in ArAr and OO collisions is larger in central collisions than in midcentral collisions. Returning to Fig. 2, we know that for central collisions as the system size decreases the eccentricities increase. Thus, there are now two competing factors that can contribute to the final v_2: A suppression effect from decreasing the system size and an enhancement effect from increasing eccentricities. In Fig. 3, when we see that all curves are very similar in 0–10% centrality, it simply is because these two competing effects roughly cancel each other out. As shown in Fig. 2, the typical eccentricity of $p+$Pb events is similar to OO events whereas the radius is divided by a factor of $\approx$2 in central collisions and $\approx$1.5 in midcentral collisions. Extrapolating our results to $p+$Pb collisions would then suggest that v_2 of $p+$Pb may be slightly smaller than the other systems but still significant in both considered centrality classes. This implies that, in the CMS $p+$Pb D mesons data, likely there is a large enough eccentricity such that v_2 does not vanish completely due to shrinking system size (although it may be that some initial flow could also influence D meson v_2 [91], we have not yet explored this possibility).

Another interesting consequence from Fig. 3 in 0–10% centrality (shown explicitly in Fig. 4) is that v_2 between $p_T =$ 2 and 5 GeV for Langevin and up to $p_T = 10$ GeV for energy loss show some sensitivity to the deformation present in the ^{129}Xe nucleus. Using a prolate nucleus, we find that there is an enhancement in this regime compared to a spherical nucleus. This is a surprising result since 0–10% is quite a wide centrality bin whereas, in the soft sector, the large deformation effects come from primarily ultracentral collisions [56,61,92–100]. Finally, although we expect a larger v_2 at a fixed $p_T \gtrsim 6$ GeV for the energy loss compared to Langevin in all systems, we find that they are both influenced by system size in a roughly equivalent way.

We also explore these effects on $v_3\{2\}(p_T)$ in Fig. 5 and find that v_3 is more sensitive to system size effects i.e., v_3 is more consistently suppressed in small systems in both centrality classes, even when there is a significant increase in ε_3. The one exception to this is 0–10% centrality for energy loss where all systems are nearly identical. Additionally, we find that the approximate universality of $v_3\{2\}(p_T)$ across centralities in PbPb collisions (see also Refs. [52,87]) is not observed in smaller systems. This approximate universality can, then, be explained by a balance between the variations in path length and eccentricity with centrality. The different response of v_2 and v_3 to system size dependence is quite interesting and may be helpful to constrain certain model parameters that could be considered in future studies.

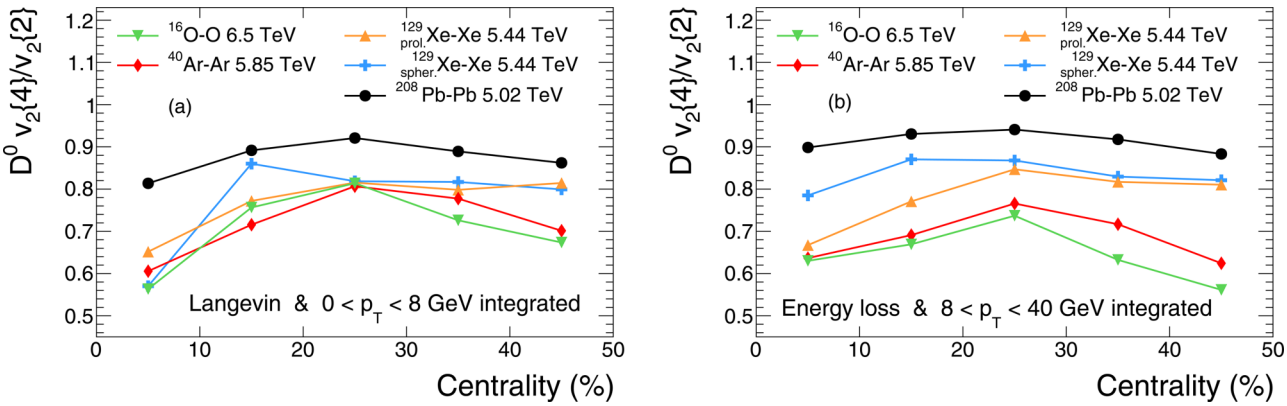

FIG. 6. (a) D^0 meson Langevin low p_T and (b) energy-loss high p_T integrated $v_2\{4\}/v_2\{2\}$ for PbPb, XeXe with spherical and prolate initial nuclei, ArAr, and OO collisions at the LHC top energies.

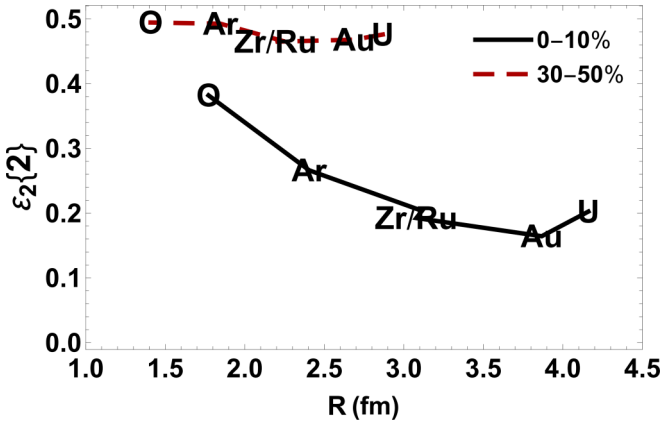

FIG. 7. $\varepsilon_2\{2\}$ vs radius for the proposed system size scan at the RHIC in 0–10% and 30–50% centrality classes.

Finally, in Fig. 6, we compare the multiparticle cumulants ratio $v_2\{4\}/v_2\{2\}$ where for the four-particle cumulant one correlates one heavy particle and three soft ones. These were first proposed in Refs. [59,69] and have yet to be measured in the heavy flavor sector. In Ref. [62], it was shown that this ratio was mostly dependent on the type of soft initial fluctuations used. In Fig. 6, we find that, generally, $v_2\{4\}/v_2\{2\}$ is suppressed with decreasing system size, which is in line with eccentricity calculations from Ref. [39]. Although the lower p_T cut is generally less sensitive to system size, high-p_T v_2 fluctuations appear to be significantly more affected by system size (whatever the considered transport model).

There has been a proposal for an intermediate system size scan at the RHIC [42] (the sPHENIX future experiment would also have these capabilities), and we anticipate a similar effect at these lower energies as well as shown in Fig. 7. To see this directly, we also calculate the $\varepsilon_2\{2\}$ vs radius relationship at the RHIC using ions that have been previously ran (^{238}U and ^{197}Au), the isobar run (^{96}Ru and ^{96}Zr), and the proposed intermediate system size scan (^{40}Ar and ^{16}O). Generally, we find the same inverse relationship between $\varepsilon_2\{2\}$ and radius in 0–10% centralities (with the exception of uranium due to its deformed structure) and the same constant eccentricities at 30–50% centralities. Thus, the proposal for a system size scan at the RHIC should see a similar effect on the D mesons as we have shown, here, but with the added consideration of a lower beam energy.

4. Conclusions. In this Rapid Communication, we make the first predictions for the D meson observables for the proposed intermediate system size scan at the LHC. We predict that $R_{AA} \to 1$ gradually as the system size is decreased with midcentral collisions approaching unity before central collisions (as expected due to their smaller system size). In midcentral collisions, we find a clear suppression of $v_n\{2\}$ in small systems, which shows the significant role played by the system size itself as the geometry of the initial conditions is nearly identical over different systems. However, in central collisions, the eccentricities become larger with a shrinking system size, which cancels out or overcomes the usual suppression effects on v_2. Thus, we predict that in central collisions $v_2\{2\}(p_T)$ will be roughly constant across the system size scan. Whereas the triangular eccentricities in central collisions increase with decreasing system size, triangular azimuthal anisotropy is more sensitive to the system size itself and, thus, one should observe a system size hierarchy. Additionally, we find that v_3 in small systems decreases with increasing centrality, whereas it is known to be roughly constant in PbPb collisions, which can now be explained by a balance between path length and eccentricity variations with centrality. Finally, although the average magnitude shifts somewhat between the two, we find that the vast majority of these features are generic for our best-fit Langevin and energy-loss models.

If confirmed, these results can help to elucidate the nature of hard probes in small systems. Heavy quarks still lose energy in the system, but as the system size path length is decreased, they lose significantly less energy. Nevertheless, this does not appear to affect v_2 in central collisions because of a significant enhancement of the ellipticity of the initial state. As was previously shown in Refs. [59,62,72,87], both the initial time and the decoupling temperature play a significant role in the v_n's in the hard sector, thus, indicating that the lifetime of the system matters as well (especially for v_3). We point out that the nearly constant v_2 across system size in central collisions falls out naturally with an initial conditions + hydrodynamics + heavy flavor Langevin or energy-loss scenario and appear to be consistent with $p+$Pb results as well (but we leave a detailed $p+$Pb study for a future paper), which may provide hints that a quark-gluon plasma could also be formed in smaller systems. However, we have not yet tested this calculation, and other studies [50] suggest that the R_{AA} do not reach unity enough in $p+$Pb to be consistent with data, showing that still remain some open questions. In future work, we hope to explore further soft-heavy correlations system size dependence, such as in Ref. [101].

Acknowledgments. We wish to thank Z. Chen, W. Li, and D. Perepelitsa for fruitful discussions and help. The authors thank Fundação de Amparo à Pesquisa do Estado de São Paulo (FAPESP) and Conselho Nacional de Desenvolvimento Científico e Tecnológico (CNPq) for support. R.K. was supported by the Region Pays de la Loire (France) under Contract No. 2015-08473. C.A.G.P. was supported by the NSFC under Grant No. 11521064, MOST of China under Project No. 2014CB845404. J.N.-H. acknowledges support from the Alfred P. Sloan Foundation, support from the U.S.-DOE Nuclear Science Grant No. DE-SC0019175, and the Office of Advanced Research Computing (OARC) at Rutgers, The State University of New Jersey for providing access to the Amarel cluster and associated research computing resources that have contributed to the results reported here.

[1] S. Chatrchyan *et al.* (CMS Collaboration), Phys. Lett. B **724**, 213 (2013).

[2] M. Aaboud *et al.* (ATLAS Collaboration), Eur. Phys. J. C **77**, 428 (2017).

[3] M. Aaboud *et al.* (ATLAS Collaboration), Phys. Rev. C **97**, 024904 (2018).
[4] G. Aad *et al.* (ATLAS Collaboration), Phys. Lett. B **725**, 60 (2013).
[5] A. M. Sirunyan *et al.* (CMS Collaboration), Phys. Rev. Lett. **121**, 082301 (2018).
[6] V. Khachatryan *et al.* (CMS Collaboration), Phys. Lett. B **742**, 200 (2015).
[7] V. Khachatryan *et al.* (CMS Collaboration), Phys. Rev. Lett. **115**, 012301 (2015).
[8] V. Khachatryan *et al.* (CMS Collaboration), Phys. Rev. C **92**, 034911 (2015).
[9] A. M. Sirunyan *et al.* (CMS Collaboration), Phys. Rev. Lett. **120**, 092301 (2018).
[10] B. B. Abelev *et al.* (ALICE Collaboration), Phys. Lett. B **726**, 164 (2013).
[11] B. B. Abelev *et al.* (ALICE Collaboration), Phys. Rev. C **90**, 054901 (2014).
[12] A. Adare *et al.* (PHENIX Collaboration), Phys. Rev. Lett. **111**, 212301 (2013).
[13] A. Adare *et al.* (PHENIX Collaboration), Phys. Rev. Lett. **114**, 192301 (2015).
[14] C. Aidala *et al.* (PHENIX Collaboration), Nat. Phys, **15**, 214 (2019).
[15] A. Adare *et al.* (PHENIX Collaboration), Phys. Rev. Lett. **121**, 222301 (2018).
[16] A. Adare *et al.* (PHENIX Collaboration), Phys. Rev. Lett. **115**, 142301 (2015).
[17] C. Aidala *et al.*, Phys. Rev. C **95**, 034910 (2017).
[18] A. Adare *et al.* (PHENIX Collaboration), Phys. Rev. C **97**, 064904 (2018).
[19] A. Adare *et al.* (PHENIX Collaboration), Phys. Rev. C **98**, 014912 (2018).
[20] C. Aidala *et al.* (PHENIX Collaboration), Phys. Rev. C **96**, 064905 (2017).
[21] C. Aidala *et al.* (PHENIX Collaboration), Phys. Rev. Lett. **120**, 062302 (2018).
[22] J. Adam *et al.* (ALICE Collaboration), Nat. Phys. **13**, 535 (2017).
[23] P. Bozek, Phys. Rev. C **85**, 014911 (2012).
[24] P. Bozek and W. Broniowski, Phys. Lett. B **718**, 1557 (2013).
[25] P. Bozek, W. Broniowski, and G. Torrieri, Phys. Rev. Lett. **111**, 172303 (2013).
[26] P. Bozek and W. Broniowski, Phys. Rev. C **88**, 014903 (2013).
[27] I. Kozlov, M. Luzum, G. Denicol, S. Jeon, and C. Gale, arXiv:1405.3976.
[28] Y. Zhou, X. Zhu, P. Li, and H. Song, Phys. Rev. C **91**, 064908 (2015).
[29] W. Zhao, Y. Zhou, H. Xu, W. Deng, and H. Song, Phys. Lett. B **780**, 495 (2018).
[30] H. Mäntysaari, B. Schenke, C. Shen, and P. Tribedy, Phys. Lett. B **772**, 681 (2017).
[31] R. D. Weller and P. Romatschke, Phys. Lett. B **774**, 351 (2017).
[32] M. Greif, C. Greiner, B. Schenke, S. Schlichting, and Z. Xu, Phys. Rev. D **96**, 091504(R) (2017).
[33] B. Schenke, S. Schlichting, P. Tribedy, and R. Venugopalan, Phys. Rev. Lett. **117**, 162301 (2016).
[34] H. Mäntysaari and B. Schenke, Phys. Rev. Lett. **117**, 052301 (2016).
[35] J. L. Albacete, H. Petersen, and A. Soto-Ontoso, Phys. Lett. B **778**, 128 (2018).
[36] P. Bozek and W. Broniowski, Phys. Rev. Lett. **121**, 202301 (2018).
[37] J. Noronha-Hostler, N. Paladino, S. Rao, M. D. Sievert, and D. E. Wertepny, arXiv:1905.13323.
[38] Z. Citron *et al.*, Report No. CERN-LPCC-2018-07, arXiv:1812.06772.
[39] M. D. Sievert and J. Noronha-Hostler, Phys. Rev. C **100**, 024904 (2019).
[40] S. H. Lim, J. Carlson, C. Loizides, D. Lonardoni, J. E. Lynn, J. L. Nagle, J. D. Orjuela Koop, and J. Ouellette, Phys. Rev. C **99**, 044904 (2019).
[41] A. V. Giannini, F. Grassi, and M. Luzum, Phys. Rev. C **100**, 014912 (2019).
[42] S. Huang, Z. Chen, J. Jia, and W. Li, Phys. Rev. C **101**, 021901 (2020).
[43] J. Adam *et al.* (ALICE Collaboration), Phys. Lett. B **754**, 81 (2016).
[44] S. Acharya *et al.* (ALICE Collaboration), J. High Energy Phys. 12 (2019) 092.
[45] D. Zigic, I. Salom, J. Auvinen, M. Djordjevic, and M. Djordjevic, Phys. Lett. B **791**, 236 (2019).
[46] S. Shi, J. Liao, and M. Gyulassy, Chin. Phys. **C43**, 044101 (2019).
[47] C. Zhang, C. Marquet, G.-Y. Qin, S.-Y. Wei, and B.-W. Xiao, Phys. Rev. Lett. **122**, 172302 (2019).
[48] C. Shen, C. Park, J.-F. Paquet, G. S. Denicol, S. Jeon, and C. Gale, *Proceedings, 25th International Conference on Ultra-Relativistic Nucleus-Nucleus Collisions* (Quark Matter 2015); Kobe, Japan, September 27-October 3, 2015, Nucl. Phys. **A956**, 741 (2016).
[49] Z.-B. Kang, I. Vitev, E. Wang, H. Xing, and C. Zhang, Phys. Lett. B **740**, 23 (2015).
[50] Y. Xu, S. Cao, G.-Y. Qin, W. Ke, M. Nahrgang, J. Auvinen, and S. A. Bass, *Proceedings, 7th International Conference on Hard and Electromagnetic Probes of High-Energy Nuclear Collisions* (Hard Probes 2015); Montréal, Québec, Canada, June 29-July 3, 2015, Nucl. Part. Phys. Proc. **276-278**, 225 (2016).
[51] R. Sharma, I. Vitev, and B.-W. Zhang, Phys. Rev. C **80**, 054902 (2009).
[52] A. M. Sirunyan *et al.* (CMS Collaboration), Phys. Rev. Lett. **120**, 202301 (2018).
[53] ATLAS Collaboration, Measurement of the long-range pseudorapidity correlations between muons and charged-particles in $\sqrt{s_{\rm NN}} = 8.16\,\text{TeV}$ proton-lead collisions with the ATLAS detector, Report No. ATLAS-CONF-2017-006 (CERN, Geneva, 2017).
[54] M. Djordjevic, S. Stojku, M. Djordjevic, and P. Huovinen, Phys. Rev. C **100**, 031901 (2019).
[55] Y. Xu *et al.*, Phys. Rev. C **99**, 014902 (2019).
[56] J. S. Moreland, J. E. Bernhard, and S. A. Bass, Phys. Rev. C **92**, 011901(R) (2015).
[57] J. Noronha-Hostler, J. Noronha, and F. Grassi, Phys. Rev. C **90**, 034907 (2014).
[58] J. Noronha-Hostler, G. S. Denicol, J. Noronha, R. P. G. Andrade, and F. Grassi, Phys. Rev. C **88**, 044916 (2013).
[59] C. A. G. Prado, J. Noronha-Hostler, R. Katz, A. A. P. Suaide, J. Noronha, and M. G. Munhoz, Phys. Rev. C **96**, 064903 (2017).

[60] P. Alba, V. Mantovani Sarti, J. Noronha, J. Noronha-Hostler, P. Parotto, I. Portillo Vazquez, and C. Ratti, Phys. Rev. C **98**, 034909 (2018).

[61] G. Giacalone, J. Noronha-Hostler, M. Luzum, and J.-Y. Ollitrault, Phys. Rev. C **97**, 034904 (2018).

[62] R. Katz, C. A. G. Prado, J. Noronha-Hostler, J. Noronha, and A. A. P. Suaide, Phys. Rev. C **102**, 024906 (2020).

[63] M. Cacciari, M. Greco, and P. Nason, J. High Energy Phys. 05 (1998) 007.

[64] M. Cacciari, S. Frixione, and P. Nason, J. High Energy Phys. 03 (2001) 006.

[65] G. D. Moore and D. Teaney, Phys. Rev. C **71**, 064904 (2005).

[66] M. Aaboud *et al.* (ATLAS Collaboration), Phys. Rev. C **98**, 044905 (2018).

[67] J. E. Bernhard, J. S. Moreland, S. A. Bass, J. Liu, and U. Heinz, Phys. Rev. C **94**, 024907 (2016).

[68] P. Moller, A. J. Sierk, T. Ichikawa, and H. Sagawa, At. Data Nucl. Data Tables **109-110**, 1 (2016).

[69] J. Noronha-Hostler, B. Betz, M. Gyulassy, M. Luzum, J. Noronha, I. Portillo, and C. Ratti, Phys. Rev. C **95**, 044901 (2017).

[70] J. Noronha-Hostler, B. Betz, J. Noronha, and M. Gyulassy, Phys. Rev. Lett. **116**, 252301 (2016).

[71] A. M. Sirunyan *et al.* (CMS Collaboration), Phys. Lett. B **776**, 195 (2018).

[72] C. Andres, N. Armesto, H. Niemi, R. Paatelainen, and C. A. Salgado, Phys. Lett. B **803**, 135318 (2020).

[73] B. Abelev *et al.* (ALICE Collaboration), Phys. Rev. Lett. **110**, 082302 (2013).

[74] CMS Collaboration, Charged particle nuclear modification factor and pseudorapidity asymmetry in pPb collisions at $\sqrt{s_{\rm NN}} = 5.02$ TeV with CMS, CMS Physics Analysis Summary, Report No. CMSPAS-HIN-12-017 (CERN, Geneva, 2013).

[75] V. Khachatryan *et al.* (CMS Collaboration), J. High Energy Phys. 04 (2017) 039.

[76] ATLAS Collaboration, D meson production and long-range azimuthal correlation in 8.16 TeV $p+$Pb collisions with ATLAS, Report No. ATLAS-CONF-2017-073 (CERN, Geneva, 2017).

[77] M. Aaboud *et al.* (ATLAS Collaboration), Eur. Phys. J. C **78**, 171 (2018).

[78] G. Bencedi (ALICE Collaboration), in *Proceedings, 51st Rencontres de Moriond on QCD and High Energy Interactions: La Thuile, Italy, 2016* (ARISF, 2016) pp. 285–288.

[79] P. Sett (PHENIX Collaboration), PHENIX measurements of nuclear modification factor of hadrons in d+Au and A+A collisions, *Proceedings, 7th International Conference on Physics and Astrophysics of Quark Gluon Plasma (ICPAQGP 2015)* (Kolkata, West Bengal, India, 2017), Vol. ICPAQGP2015, pp. 091.

[80] T. Todoroki (STAR Collaboration), Nucl. Phys. A **967**, 572 (2017).

[81] X.-N. Wang, Phys. Rev. C **63**, 054902 (2001).

[82] M. Gyulassy, I. Vitev, and X. N. Wang, Phys. Rev. Lett. **86**, 2537 (2001).

[83] J. Liao and E. Shuryak, Phys. Rev. Lett. **102**, 202302 (2009).

[84] J. Jia, W. A. Horowitz, and J. Liao, Phys. Rev. C **84**, 034904 (2011).

[85] K. C. Zapp, Phys. Lett. B **735**, 157 (2014).

[86] B. Betz and M. Gyulassy, J. High Energy Phys. 08 (2014) 090; 10 (2014) 043.

[87] M. Nahrgang, J. Aichelin, S. Bass, P. B. Gossiaux, and K. Werner, Phys. Rev. C **91**, 014904 (2015).

[88] J. Xu, J. Liao, and M. Gyulassy, Chin. Phys. Lett. **32**, 092501 (2015).

[89] Y. Xu, J. E. Bernhard, S. A. Bass, M. Nahrgang, and S. Cao, Phys. Rev. C **97**, 014907 (2018).

[90] S. Cao *et al.*, Phys. Rev. C **99**, 054907 (2019).

[91] Y. Sun, G. Coci, S. K. Das, S. Plumari, M. Ruggieri, and V. Greco, Phys. Lett. B **798**, 134933 (2019).

[92] W. Broniowski and E. Ruiz Arriola, Phys. Rev. Lett. **112**, 112501 (2014).

[93] L. Adamczyk *et al.* (STAR Collaboration), Phys. Rev. Lett. **115**, 222301 (2015).

[94] H. Wang and P. Sorensen (STAR Collaboration), Nucl. Phys. A **932**, 169 (2014).

[95] A. Goldschmidt, Z. Qiu, C. Shen, and U. Heinz, Phys. Rev. C **92**, 044903 (2015).

[96] M. Rybczyński, M. Piotrowska, and W. Broniowski, Phys. Rev. C **97**, 034912 (2018).

[97] B. Schenke, C. Shen, and P. Tribedy, Phys. Rev. C **99**, 044908 (2019).

[98] CMS Collaboration, Pseudorapidity distributions of charged hadrons in XeXe collisions at $\sqrt{s_{\rm NN}} = 5.44$ TeV, CMS Physics Analysis Summary, Report No. CMS-PAS-HIN-17-006 (CERN, Geneva, 2018).

[99] S. Acharya *et al.* (ALICE Collaboration) Phys. Lett. B **784**, 82 (2018).

[100] ATLAS Collaboration, Measurement of the azimuthal anisotropy of charged particle production in Xe + Xe collisions $\sqrt{s_{\rm NN}} = 5.44$ TeV with the ATLAS detector, Report No. ATLAS-CONF-2018-011 (CERN, Geneva, 2018).

[101] S. Plumari, G. Coci, S. K. Das, V. Minissale, and V. Greco, Nucl. Phys. A **982**, 655 (2019).